# In Vivo Prostate Magnetic Resonance Spectroscopic Imaging Using Two-Dimensional J-Resolved PRESS at 3 T

Dong-hyun Kim,[1]* Daniel Margolis,[1] Lei Xing,[2] Bruce Daniel,[1] and Daniel Spielman[1]

**In vivo magnetic resonance spectroscopic imaging of the prostate using single-voxel and multivoxel two-dimensional (2D) *J*-resolved sequences is investigated at a main magnetic field strength of 3 T. Citrate, an important metabolite often used to aid the detection of prostate cancer in magnetic resonance spectroscopic exams, can be reliably detected along with the other metabolites using this method. We show simulations and measurements of the citrate metabolite using 2D *J*-resolved spectroscopy to characterize the spectral pattern. Furthermore, using spiral readout gradients, the single-voxel 2D *J*-resolved method is extended to provide the spatial distribution information as well all within a reasonable scan time (17 min). Phantom and in vivo data are presented to illustrate the multivoxel 2D *J*-resolved spiral chemical shift imaging sequence. Magn Reson Med 53:1177–1182, 2005. © 2005 Wiley-Liss, Inc.**

**Key words: magnetic resonance spectroscopic imaging; prostate cancer; spiral readout gradients; 2D *J*-resolved spectroscopy; citrate; polyamine**

In addition to the morphologic information provided by magnetic resonance imaging, the additional information gained using magnetic resonance spectroscopy (MRS) and magnetic resonance spectroscopic imaging (MRSI) increases the specificity of the examination for prostate cancer (PCa). In these examinations, the ratio of (choline + creatine) to citrate is often regarded as a marker for PCa (1). To date, MRSI protocols for PCa detection have been well established at a main magnetic field strength of 1.5 T (2).

The advent of higher field strength scanners provides the potential for improvement over 1.5-T systems due to the inherent increase in the signal-to-noise ratio (SNR). For PCa exams using MRS/MRSI methods, this advantage can be exploited in various forms, which include using higher spatial resolution acquisitions to increase the accuracy of localization of the cancerous tissues (3). Scan times can also be made shorter compared to 1.5 T for the same SNR, thereby reducing the overall MR examination time. The extension of 1.5-T MRS/MRSI protocols for usage in 3-T PCa can therefore have potential merits.

However, the process of advancing to higher field strength requires several considerations. For clinical prostate examinations using spectroscopic techniques, one of the issues that arise involves the detection of the citrate metabolite. Strong coupling of the AB system of citrate induces echo-time-dependent modulations of the signal response, which differs significantly with field strength (4,5). One method which exploits the echo time dependencies is the 2D *J*-resolved spectroscopic sequence (6–8). Acquisitions at incremental echo times can be gathered to obtain the coupling information of such metabolites. Information of uncoupled metabolites can also be gathered. Another advantage of using 2D *J*-resolved sequences in the case of prostate is the potential to separate the polyamine metabolite from the creatine and choline peaks (9,10). The three metabolites resonate at similar frequencies, which make them hard to differentiate using normal acquisitions. But, since the polyamines are also strongly coupled, the 2D *J*-resolved method can provide additional information, which can be used to distinguish between creatine and choline. In addition, 2D *J*-resolved spectroscopy has been used to reduce sideband artifacts for applications in the brain and regions outside of the brain such as the breast (11,12). Finally, the acquisitions from multiple echo times can also help determine the $T_2$ values of metabolites of interest in addition to water.

To take full advantage of this method, collecting the spatial distribution information of the metabolites will be preferred over single-voxel techniques. Although phase encoded MRSI methods have been used in obtaining the spatial information, this can be problematic when combining with the 2D *J*-resolved method since the minimum total scan time will be increased proportional to the number of echo time steps used. Therefore, a different approach that can reduce the minimum total scan time needs to be established. One of the spatial encoding methods that achieve such characteristic is the spiral readout MRSI (13). Using spiral MRSI, the spatial coverage can be controlled with high efficiency, thereby significantly decreasing the minimum total scan time compared to the phase encoded method. The additional time available can therefore be used to gather the 2D *J*-resolved spectroscopic data (14,15).

This work involves the study of 2D J-resolved single-voxel and multivoxel spectroscopic acquisition methods targeted for clinical application of PCa detection. We first explore the use of a 2D *J*-resolved single-voxel spectroscopic sequence to illustrate the detection of the citrate metabolite and to observe the characteristics of the *J*-coupled spectral pattern. Multivoxel 2D *J*-resolved acquisitions are performed using spiral-based MRSI.

[1]Department of Radiology, Stanford University, Stanford, California, USA.
[2]Department of Radiation Oncology, Stanford University, Stanford, California, USA.

Grant sponsor: Lucas Foundation; Grant sponsor: NIH; Grant numbers: CA 48269, RR09784, and 1R01CA098523–01A1; Grant sponsor: Department of Defense; Grant number: DAMD17–03-1–0023.

*Correspondence to: Dong-hyun Kim, Radiological Science Laboratory at the Lucas MRS/I Center, Department of Radiology, Stanford University, 1201 Welch Road, Stanford, CA 94305-5488, USA. E-mail: dhkim@mrsc.ucsf.edu

Received 4 August 2004; revised 10 December 2004; accepted 15 December 2004.

DOI 10.1002/mrm.20452
Published online in Wiley InterScience (www.interscience.wiley.com).

## METHODS

Simulations and phantom measurements were conducted assuming a 2D *J*-resolved acquisition using a PRESS excitation scheme. For the simulations, we solved the full density matrix of strongly coupled two-spin systems with nonselective 180° pulses. The timing of the PRESS sequence was assumed to be 90°–[$t_{int}$]–180°–[$t_1/2$]–180°–[$t_1/2 - t_{int}$]–$t_2$ (acquire), where $t_{int}$ was 10 ms. The *J*-coupling constant was assumed to be 15.4 Hz with a chemical shift value of 0.12 ppm (= 16.6 Hz at 3 T) (16). Also, the $T_2$ was assumed to be 200 ms with a line width of 10 Hz. For the actual single-voxel 2D *J*-resolved measurements, a phantom composed of citrate, creatine, and choline metabolites was used to emulate the existence of cancerous tissue. In both cases, the echo time spacing was adjusted to be 7.8 ms for a total of 64 steps from 35 to 534 ms in the F1 domain (Fourier domain corresponding to $t_1$ dimension). This resulted in a 2-Hz spectral resolution with a bandwidth of 128 Hz in the F1 domain. The spectral bandwidth in the F2 domain (Fourier domain corresponding to $t_2$ dimension) was 5000 Hz with 2048 data point acquisitions.

In vivo data were collected from a patient suspicious for recurrent PCa using the single-voxel 2D *J*-resolved technique. Single-voxel 2D *J*-resolved spectroscopic data using the PRESS sequence were acquired from two different regions near the peripheral zone of the prostate. All PRESS sequences were preceded by CHESS water suppression and very selective saturation pulses for spatial saturation (17). The voxel size chosen was 1 × 1.12 × 1.08 cm = 1.2 cc. Four acquisitions were averaged per incremental echo time for a total scan time of 8 min (TR = 2 s) for each voxel.

Multivoxel 2D *J*-resolved data using spiral MRSI were also acquired. A detailed description of the spiral MRSI sequence can be found in Ref. 14. First, phantom data were collected to demonstrate the feasibility of obtaining spatial as well as the coupling information followed by in vivo data collection. Spiral readout gradients were applied to a PRESS excitation sequence. The spirals were designed using the formula given by Glover (18). A 32 × 32 spatial matrix covering a 24-cm field of view was used. Sixteen spatial interleaves of the spirals were used to acquire the required *k*-space. The number of spirals repeated during each acquisition was 256 lobes, which resulted in a 950-Hz spectral bandwidth in the F2 domain. Sixteen different echo times starting from 35 to 285 ms with 15.6-ms intervals were used to collect F1 domain information, which accounted for F1 spectral resolution of 4 Hz and a bandwidth of 64 Hz. Collected data were processed by first gridding in the $k_x$, $k_y$, and $t_2$ domains followed by a four-dimensional FT into the *x*, *y*, F1, and F2 domains. In summary, each of the 32 × 32 reconstructed voxels had 16 spectra, which covers the F1 dimension from *J*(−32) Hz to *J*(28) Hz. The nominal voxel size was 0.59 cc while the total scan time to acquire the necessary *k*-space and the $t_1$ space data was 17 min (TR = 2 s).

For the multivoxel 2D *J*-resolved experiment, phantom data were acquired using the head coil while in vivo data were collected with the body coil for excitation followed by a rigid endorectal coil for signal reception. A phantom comprised of creatine, choline, and citrate solution was built for this study, which was surrounded by lipids to confirm the lipid suppression capabilities. For the in vivo exams, a high-resolution (512 × 512) $T_2$-weighted anatomic image was obtained and a region of interest covering most of the prostate was selected for the PRESS sequence. To date, seven patients who were suspicious of prostate cancer were referred to by a pathologist and imaged using

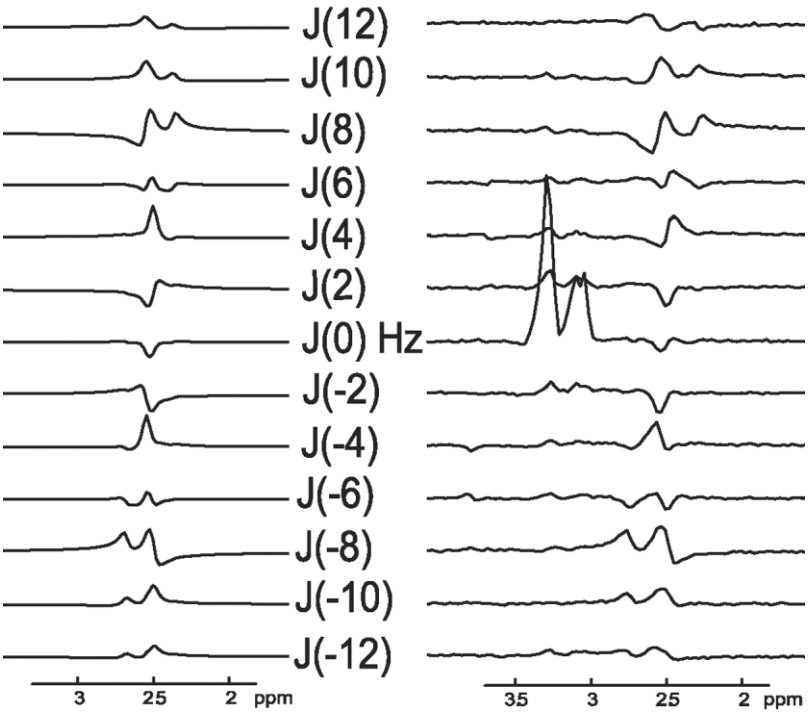


FIG. 1. 2D *J*-resolved spectra obtained from simulations (left) and phantom measurements (right) at 3 T. The echo time interval was 7.8 ms starting from 35 ms for 64 steps. Choline and creatine metabolites were added for the phantom measurement. Due to the modulations as a function of echo time, the 2D *J*-resolved spectra show a strong signal from the citrate metabolite at reconstructed lines beyond the *J*(0) Hz line for both simulated and measured data with similar spectral patterns. In this respect, the detection of the citrate resonance can be made outside of the *J*(0) Hz line using the 2D *J*-resolved acquisition.

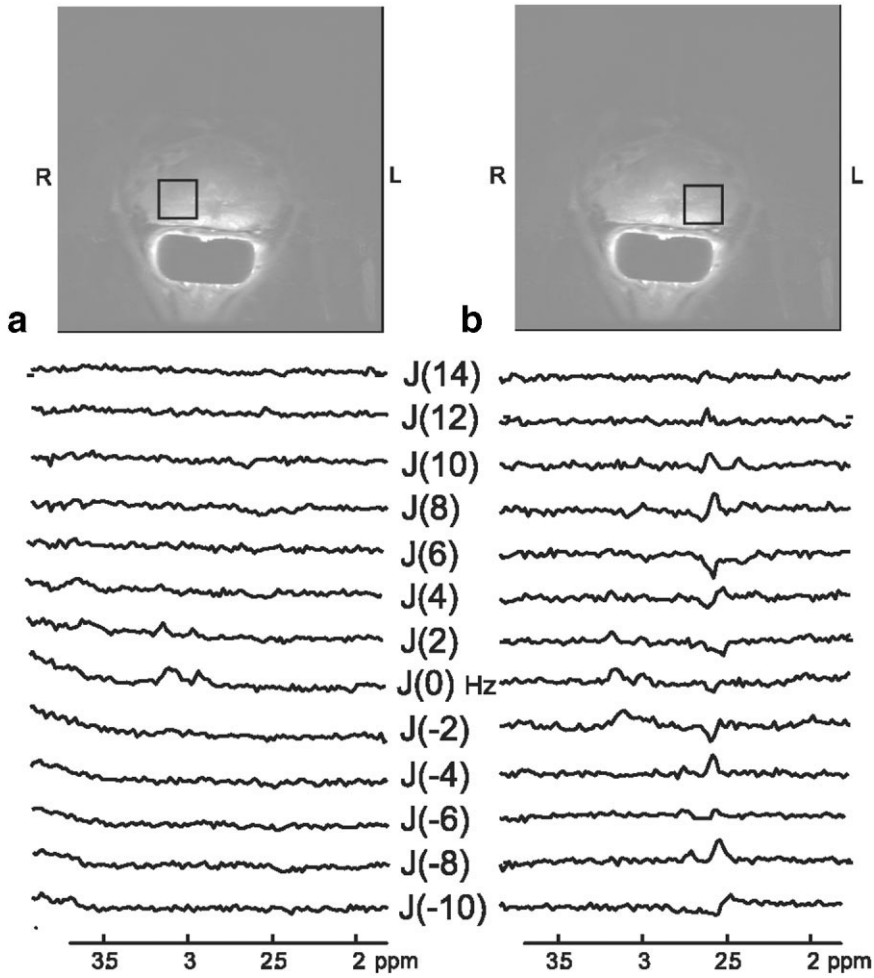


FIG. 2. Single-voxel 2D *J*-resolved spectroscopy results obtained in vivo from a subject suspicious of recurrent PCa. Two voxels were selected for the examination as shown in the $T_2$-weighted images. The reconstructed spectra of several F1 lines are shown. In (**a**), even though the presence of creatine and choline metabolites is evident, there is no visible citrate. As for the region shown in (**b**), the citrate is visible (2.6 ppm region from $J(-10)$ to $J(12)$ Hz line) in the spectra while other metabolites are also present. This shows that the 2D *J*-resolved spectroscopy can be useful for in vivo detection of citrate.

a 3 T GE Signa scanner (GE Health Care, Waukesha, WI). All in vivo studies were conducted under IRB guidelines and with informed consent.

## RESULTS

Figure 1 shows the simulated 2D *J*-resolved citrate spectra (left) along with the reconstructed 2D *J*-resolved data acquired with a phantom (right) using the single-voxel 2D *J*-resolved acquisition. Spectra corresponding to the F1 domain in the range of $J(-12)$ to $J(12)$ Hz were extracted where most of the energy is concentrated. In both cases, due to the modulations occurring as a function of echo time, resonances are clearly seen beyond the $J(0)$ line for the citrate metabolite. Individual spectra from each F1 line reveal the similarity of the patterns between the simulated and measured results of the citrate. The $J(0)$ line, also referred to as the TE-averaged line, has a slight negative peak at the citrate position, which is due to the strong negative peaks at echo times ranging from 60 to 120 ms.

Two single-voxel 2D *J*-resolved spectra from an in vivo subject are presented in Fig. 2. The patient had a prior history of prostatic adenocarcinoma, which was treated by external beam radiation. The two regions that were selected are shown in the anatomic $T_2$-weighted images along with the resulting *J*-resolved spectra. The spectra obtained from the right side of the subject (Fig. 2a) displays negligible citrate metabolite intensity compared to the creatine and choline resonances located near the 3.0-ppm region. In comparison, the spectra from the left side of the subject (Fig. 2b) reveal the presence of citrate as seen from the modulations occurring in the reconstructed F1 lines along with the creatine and choline metabolites. These two comparisons show that with the 2D *J*-resolved acquisition method, the strongly coupled citrate metabolite can be resolved while the presence of other metabolites can be established. Even though the number of radiofrequency (RF) phase cycling steps has been reduced to 4 in this case, strong residual signal from outside of the PRESS box is not observed.

In Fig. 3, results obtained from the multivoxel 2D *J*-resolved sequence via spiral MRSI are shown. In Fig. 3a, an image of the phantom that was used for the experiment is given. In Fig. 3b, the metabolite spectra corresponding to the voxel selected in Fig. 3a are given. We extracted the TE-averaged line from each reconstructed voxel and manually phased them. The TE-averaged spectra show the well-resolved spatial distribution of the metabolites with a slight negative peak of the citrate as in the case of the single-voxel experiment. Spatial saturation pulses eliminated most of the lipids, as can be seen from the absence of any sidebands arising from the lipids. In Fig. 3c, lines from

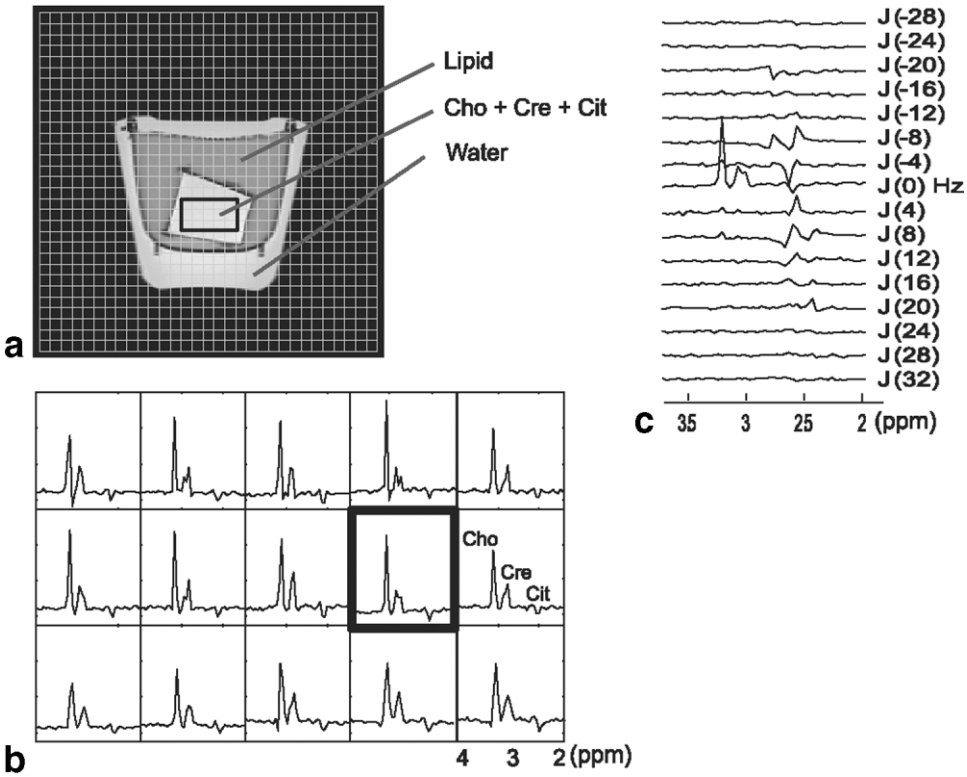


FIG. 3. Phantom results using spiral based multivoxel 2D *J*-resolved MRSI. A metabolite phantom surrounded by lipid and water was used (**a**). In (**b**), the metabolite spectra corresponding to *J*(0) Hz are displayed from the selected voxels shown in (a). The TE-averaged spectra show the well-resolved spatial distribution of the metabolites. In (**c**), all the reconstructed F1 lines for the voxel highlighted in (b) are shown. The F1 domain lines clearly depict the presence of citrate near the 2.5-ppm region.

*J*(−28) to *J*(32) Hz that were reconstructed for the voxel highlighted in Fig. 3b are shown. The *J*-resolved F1 domain lines clearly depict the presence of citrate located near the 2.5-ppm region.

Figure 4 shows spiral readout 2D *J*-resolved MRSI results obtained from an in vivo subject who had been reported as having a Gleason score of 3 + 3. The $T_2$-weighted image is shown in Fig. 4a with a grid representing the displayed voxels shown in Fig. 4b and c. Reconstructed spectra corresponding to the TE-averaged lines are given in Fig. 4b. As with the case of the phantom experiment, the TE-averaged line largely represents spectra from metabolites that are uncoupled. This is illustrated by the existence of choline and creatine metabolites that can be seen near the middle region of the displayed voxels. In Fig. 4c, the spectra corresponding to *J*(8) Hz are displayed where the citrate metabolite can be resolved. This is illustrated near the upper left region of the prostate where several voxels show a peak near the 2.5 ppm region, which corresponds to the citrate metabolite. For several voxels, however, lipid contamination can be visible near the 2.5-ppm region, which compromised the detection of citrate.

Figure 5 shows spiral readout 2D *J*-resolved MRSI results obtained from another in vivo subject who had been reported as having adenocarcinoma of the prostate with a Gleason score of 3 + 4. The TE-average lines in Fig. 5a show voxels of signal contributing from creatine and choline as well as polyamines residing in *J*(0) Hz. In Fig. 5c, the spectra corresponding to *J*(8) Hz line are displayed. The spectra show clear visualization of the citrate metabolite. In addition, polyamines are seen to be resolved as well. Of the seven patients examed, five patients had observable signal from any of the metabolites of interest.

## DISCUSSION

We have shown the application of a 2D *J*-resolved PRESS sequence, which can aid the detection of PCa at the field strength of 3 T. In the first part of the paper, simulations and phantom measurements showing the characteristics of the citrate metabolite resonance for 2D *J*-resolved single-voxel acquisitions were illustrated, which showed the strong dependency with echo time due to its strong coupling. In the second part spiral readout gradients were applied to the 2D *J*-resolved PRESS sequence to obtain additional spatial distribution information. The efficiency of the spiral *k*-space trajectory makes it possible to cover the whole *k*-space within a reasonable scan time.

For a truly feasible clinical protocol to be implemented, several prerequisites need to be established, however. It is important for a good spatial suppression pulse to be used so that there are no aliasing or ringing artifacts. This problem has been demonstrated from the in vivo exam where lipid sidebands interfered with the detection of metabolites. This result is in comparison with the phantom results where good lipid suppression was accomplished. For the phantom experiment, a head coil with a relatively homogeneous RF profile and low power was used, whereas this was not the case for the in vivo exam, which used the body coil for excitation. Another important prerequisite is the main field homogeneity. The presence of air inside the endorectal coil or near the prostate region can degrade the homogeneity, leading to line broadening and potential overlap of the choline and creatine metabolites as seen in the in vivo example.

In this study, we addressed the issue of strong coupling citrate peak using a 2D *J*-resolved spectroscopic acquisi-

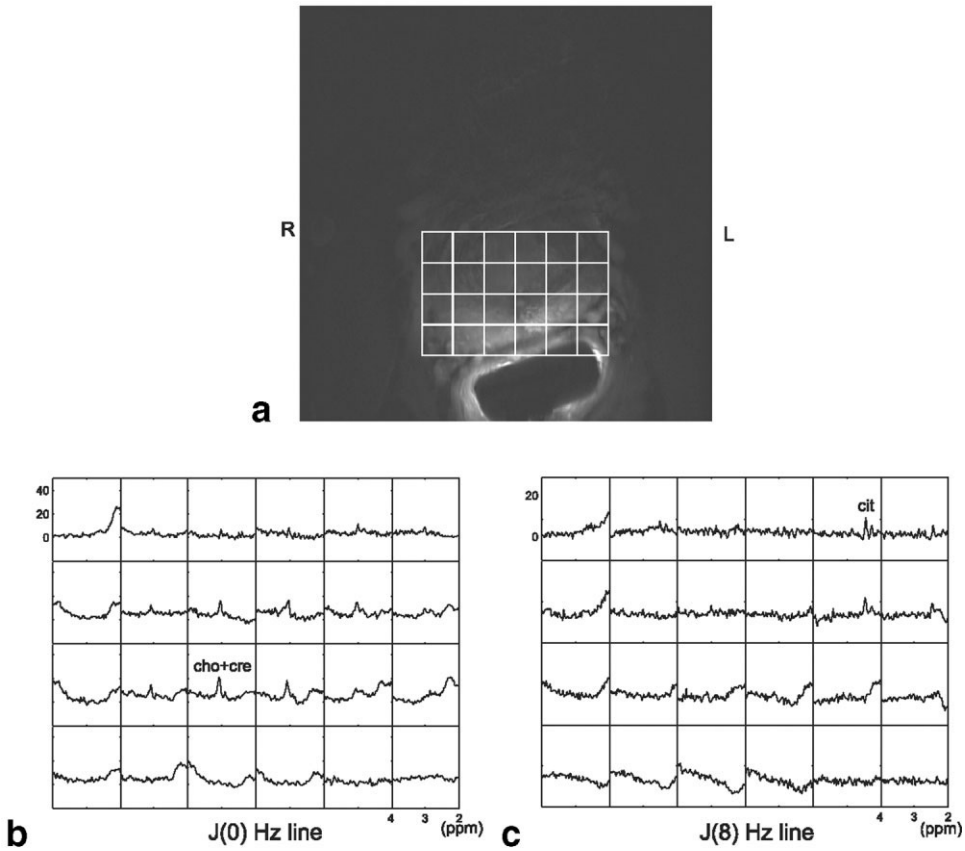


FIG. 4. Results obtained from a patient diagnosed with prostate cancer with a Gleason score 3 + 3 using spiral-based 2D *J*-resolved MRSI. (**a**) $T_2$-weighted image with a grid representing the displayed voxels. (**b**) Reconstructed spectra corresponding to the *J*(0) Hz lines. The existence of choline and creatine metabolites can be seen near the middle region of the displayed voxels. (**c**) Spectra corresponding to *J*(8) Hz line from F1 domain. Several voxels show a peak near the 2.5-ppm region at the upper left region, which corresponds to citrate. Lipid contamination can be visible near the 2.5-ppm region for several voxels.

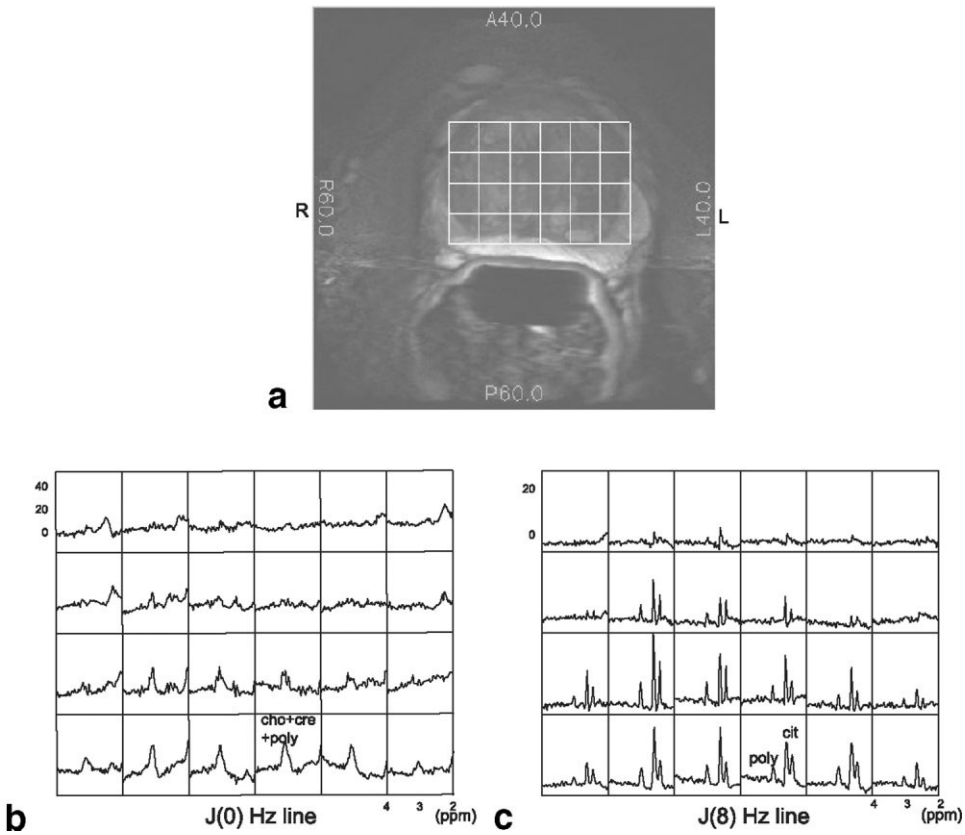


FIG. 5. Results obtained from a patient diagnosed with adenocarinoma of the prostate with a Gleason score 3 + 4 using spiral-based 2D *J*-resolved MRSI. (**a**) $T_2$-weighted image with a grid representing the displayed voxels. (**b**) Reconstructed spectra corresponding to the *J*(0) Hz lines. The coexistence of choline, creatine, and polyamine metabolites can be seen. (**c**) Spectra corresponding to the *J*(8) Hz line. Several voxels show a clear peak near the 2.5-ppm region corresponding to citrate. Polyamines can also be observed for several voxels around the 3.1-ppm region.

tion sequence. This can be dealt with in a different way as recently shown using a *J*-refocused sequence (19). One of the advantages of using the 2D *J*-resolved method includes the potential to detect changes in the citrate coupling constant, which can be used as another marker for PCa. This coupling constant is believed to be related to the zinc concentration, which is directly related to presence of PCa (20). In addition, any information obtained from the second spectral dimension, for example, from the polyamines as seen, can add to the physiologic information of the prostate tissue (9). On the negative side, a *J*-refocused scheme would require many fewer acquisitions and can achieve better SNR due to a shortened TE.

## CONCLUSION

Single-voxel and multivoxel 2D *J*-resolved spectroscopy methods have been demonstrated for in vivo prostate at field strength of 3 T. Using the 2D *J*-resolved method, strong coupling of citrate can be well resolved. For multivoxel 2D *J*-resolved spectroscopic imaging, spiral-based readout sequences are used, which enable data acquisition within a reasonable scan time.

## REFERENCES


1. Scheidler J, Hricak H, Vigneron DB, Yu KK, Sokolov DL, Huang RL, Zaloudek CJ, Nelson SJ, Carroll PR, Kurhanewicz J. 3D $^{1}$H-MR spectroscopic imaging in localizing prostate cancer: clinico-pathologic study. Radiology 1999;213:473–480.
2. Kurhanewicz J, Vigneron DB, Hricak H, Narayan P, Carroll P, Nelson SJ. Three-dimensional $^{1}$H MR spectroscopic imaging of the in situ human prostate with high (0.24–0.7 $cm^3$) spatial resolution. Radiology 1996; 198:795–805.
3. Vigneron DB, Chen A, Cunningham C, Xu D, Hurd R, Sailasuta N, Pauly J, Nelson S, Kurhanewicz J. High resolution 3D MR spectroscopic imaging and J-resolved MRS of the prostate at 3 Tesla. In: Proceedings of the 12th Annual Meeting of ISMRM, Kyoto, Japan, 2004. p 386.
4. Wilman AH, Allen PS. The response of the strongly coupled AB system of citrate to typical $^{1}$H MRS localization sequences. J Magn Reson B 1995;107:25–33.
5. Mulkern RV, Bowers JL, Peled S, Kraft RA, Williamson DS. Citrate signal enchancement with a homonuclear J-refocusing modification to double-echo PRESS sequences. Magn Reson Med 1996;36:775–780.
6. Aue WP, Karhan J, Ernst RR. Homonuclear broadband decoupling and two-dimensional J-resolved NMR spectroscopy. J Chem Phys 1976;64: 4226.
7. Thomas MA, Ryner L, Mehta M, Turski P, Sorenson JA. Localized 2D J-resolved $^{1}$H MR spectroscopy of human brain tumors in vivo. J Magn Reson Imaging 1996;6:453–459.
8. Dreher W, Leibfritz D. On the use of two-dimensional-J NMR measurements for in vivo proton MRS: Measurements of homonuclear decoupled spectra without the need for short echo time. Magn Reson Med 1995;34:331–337.
9. Swanson MG, Vigneron DB, Tran TC, Sailasuta N, Hurd RE, Kurhanewicz J. Single-voxel oversampled J-resolved spectroscopy of in vivo human prostate tissue. Magn Reson Med 2001;45:973–980.
10. Yue K, Marumoto A, Binesh N, Thomas MA. 2D JPRESS of human prostates using an endorectal receiver coil. Magn Reson Med 2002;47: 1059–1064.
11. Hurd RE, Gurr D, Sailasuta N. Proton spectroscopy without water suppression: the oversampled J-resolved experiment. Magn Reson Med 1998;40:343–347.
12. Bolan PJ, DelaBarre L, Baker EH, Merkle H, Everson LI, Yee D, Garwood M. Eliminating spurious lipid sidebands in $^{1}$H MRS of breast lesions. Magn Reson Med 2002;48:215–222.
13. Adalsteinsson E, Irarrazzabal P, Topp S, Meyer C, Macovski A, Spielman DM. Volumetric spectroscopic imaging with spiral-based k-space trajectories. Magn Reson Med 1998;39:889–898.
14. Adalsteinsson E, Spielman DM. Spatially resolved two-dimensional spectroscopy. Magn Reson Med 1999;41:8–12.
15. Hiba B, Serduc R, Provent P, Farion R, Remy C, Ziegler A. 2D J-resolved spiral spectroscopic imaging at 7 T: application to mobile lipid mapping in a rat glioma. Magn Reson Med 2004;52:658–662.
16. Schick F, Bongers H, Kurz S, Jung W, Pfeffer M, Lutz O. Localized proton MR spectroscopy of citrate in vitro and of the human prostate in vivo at 1.5T. Magn Reson Med 1993;29:38–43.
17. Tran TC, Vigneron D, Sailasuta N, Tropp J, LeRoux P, Kurhanewicz J, Nelson SJ, Hurd R. Very selective suppression pulses for clinical MRSI studies of brain and prostate cancer. Magn Reson Med 2000;43:23–33.
18. Glover GH. Simple analytic spiral k-space algorithm. Magn Reson Med 1999;42:412–415.
19. Cunningham CH, Marjanska M, Chen AP, Xu D, Pauly JM, Sailasuta N, Hurd RE, Kurhanewicz J, Garwood M, Vigneron DB. Sequence design incorporating the LASER technique for prostate MRSI at high field. In: Proceedings of the 12th Annual Meeting of ISMRM, Toronto, Canada, 2003. p 682.
20. Van der Graaf M, Heerschap A. Effect of cation binding on the protonchemical shifts and the spin-spin coupling constant of citrate. J Magn Reson B 1996;112:58–62.